Int. J. Electrochem. Sci., 16 **(2021)** Article ID: 210357, doi: 10.20964/2021.03.32

International Journal of ELECTROCHEMICAL SCIENCE
www.electrochemsci.org

Short Communication

Application of Electrochemically Synthesized Zinc Oxide Nanorods/Fava Bean Starch biocomposite in Food Active Packaging

Heqin Xing[1,2], *Tiehua Zhang*[1,2], *Fengguang Pan*[1,2], *Jingbo Liu*[1,2,*]

[1] College of Food Science and Engineering, Jilin University, Changchun, 130062, China
[2] Key Laboratory of Nutrition and Functional Food of Jilin Province, Jilin University, Changchun, 130062, China
[*]E-mail: jlu_jingboliu@aliyun.com

Received: 26 October 2020 / *Accepted:* 19 December 2020 / *Published:* 31 January 2021

Fava bean starch (FBS) nanocomposite films with ZnO nanorods (NRs) filler were successfully prepared and characterized. ZnO NRs powder was synthesized using a simple electrochemical method in large-scale production. ZnO NRs as a physical cross-linking to reduce the starch thermal decomposition indicated significant improvement in the thermal stability of biopolymer samples. A huge difference in the electrical conductivity and relative dielectric constant was observed by increasing the ZnO concentration in the FBS matrix. The localization of charge carriers in the ZnO/FBS biopolymers can result in the enhancement of the antibacterial properties of starch-based polymer through the electrostatic discharge between ZnO NRs and bacteria. Biocomposite films incorporated with ZnO NRs revealed excellent antibacterial activities and thus can be used as an active packaging material to ensure safety of packaged foods and pharmaceuticals.

Keywords: ZnO/FBS biopolymer films; Electrochemical method; Dielectric properties; Thermal properties

1. INTRODUCTION

Fava beans have a long history of cultivation in ancient Egypt, Greece and Rome and also reached China in 2800 BC. Fava bean starch (FBS) can be produced and accessed almost anywhere in the world which could be a great advantage for related industries. Now, most of the materials used in industry is created from petroleum-based plastic materials because of the relatively opportune use, high durability, and low cost [1, 2]. However, due to the increasing oil price, many researchers are working on the expansion of recyclable materials by using biocomposites to alternate plastic materials [3-6]. Therefore, renewable-based strategies can lead to severe reduction in greenhouse gas emissions and non-renewable source consumption. Among the natural composites, starch is a promising material

that is biodegradable and a renewable resource which is commonly readily available and low cost [7, 8]. Due to poor processing, mechanical, barrier properties of biopolymer materials, and the higher cost of production compared to plastic products, biomaterials in industry have not been widely used [9, 10]. Many researchers are working on homogenizing bio polymer with a variety of nanofiller materials that led to the development of the mechanical, gas barrier, and physical properties of the matrix [11-13]. Among these nanofillers, ZnO nanostructures have a large surface area, optical transparency, high surface energy, and considerable mechanical and thermal properties that make them a potential candidate as polymer matrix boosters [14-21]. Moreover, ZnO in nanoscale, for example, nanoparticle structure incorporated with various biopolymers, has presented in various agricultural, drug release, medical and packaging applications. The development of bionanocomposites is essential not only to decrease environmental issues but also to develop renewable-based strategies. In this study, a simple and novel technique has been used for the large-scale synthesis of ZnO nanorod powder by a factory ZnO furnace at the temperature of 1300 °C. ZnO nanostructures were used as fillers to make ZnO/FBS biopolymer matrices. The nanocomposites were considered for their electrical, optical and thermal stability properties.

2. MATERIALS AND METHODS

To synthesis ZnO nanorods by electrochemical process, 250 ml of the electrolyte solution was put in a 300 ml electrochemical cell. The electrolyte mixtures have been prepared by mixing choline chloride: ethylene glycol (1:2 molar ratio), 0.01M $Zn(CH_3COO)_2{\cdot}2H_2O$ and 1.5 mL/L H_2O_2. Conductivity and pH of the electrolyte solution were attuned using KCl and 1 M NaOH, respectively. Zn electrodes were immersed in the electrolytic cell. The distance between the anode and cathode electrodes was approximately 2 cm. The electrodes were connected to the DC power source. The voltage and time were kept at 5V for 1 h at room temperature, respectively. Finally, the aqueous solution was subjected to a centrifugal force at 7000 rpm at 5 °C for 20 min. The white yield attained was further rinsed with DI water dried at 90 °C for one day.

Prepared ZnO NRs were added to deionized (DI) water at various concentrations. The solution was heated at a temperature of 70 °C with constant stirring to totally dissolve the ZnO NRs for approximately 45 min. Then, the solution was placed for 25 min in a lab ultrasonic cleaner. The mixture was cooled at room temperature and used to supply 5 wt% aqueous FBS. A combination of glycerol and sorbitol (1:3) was added at 40% of whole solid as plasticizers. The biocomposite films were heated to temperature of 55 °C and kept for gelatinization to 45 minutes. When the starch gelatinized, the mixture was cooled to ambient temperature. One portion (90 g of starch) was spread onto Perspex plates with the dimensions 150 mm×150 mm. The biocomposite matrices were dried at room temperature with relative humidity (RH) of 50% for 24 h. Non-fillers samples were provided with the same plasticizers. In order to investigate more, dried films were maintained at approximately 52% RH and 25 ° C in a desiccator.

The films were considered by transmission electron microscopy (TEM, Philips CM12, FEI, CO) and FE scanning electron microscopy (FESEM, FEI Sirion 200) analyses. Cyclic voltammetry (CV) measurements were done in –0.3 to 0.5 V potential range at a 30 mVs^{-1} scan rate.

The dielectric permittivity of ZnO/FBS nanocomposites was recorded in the frequency range between 0.001 and 10000 Hz (Agilent 4284a Precision LCR meter).

The thermal stability of bionanocomposite films were investigated by aPyris 1 TGA thermogravimetric analyzer. The sample temperature was increased from 50 °C to 600 °C at a 10 °C/min rate under the N flow of 20 mL/min to prevent thermo-oxidative reactions.

The antimicrobial effects of the film against Staphylococcusaureus (*S. aureus*) and Escherichia coli (*E. coli*) were determined by the usage of inhibition in a solid media zone. Mueller Hinton (Merck, Darmstadt, Germany) agar plates were rubbed with 100 mL of inoculum with about 10^6–10^7CFU/mL of tested bacteria. Disc-shaped film samples were placed on these discs. Incubation of these plates took place at 37 °C in a subsequent manner for a day under mild shaking. The diameter of the inhibition zone of the bacterial growth around the film was used to calculate the antimicrobial activity of the films.

3. RESULTS AND DISCUSSION

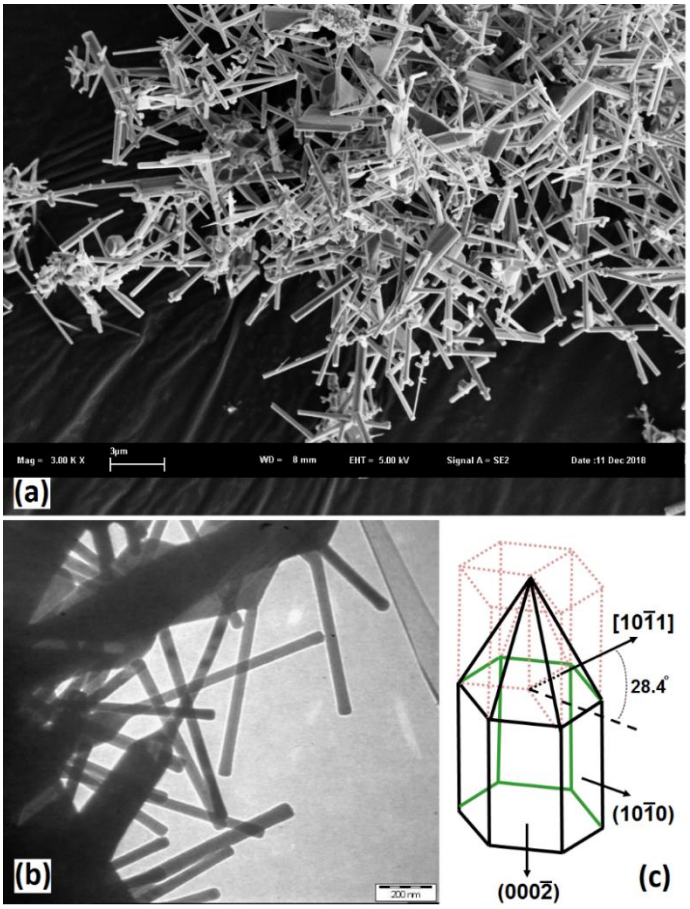

Figure 1. (a) FESEM micrographs of ZnO NRs, (b) HRTEM of a ZnO NRs cluster and (c) ZnO crystal simulation.

Fig. 1a indicates the FESEM image of ZnO nanostructure powders synthesized by gas-phase technique. The Fig. 1a obviously showed that the as-grown products present rod-shaped structures. The length distribution of the ZnO NRs shows that most NRs have lengths between 0.5 and 2 μm. Fig. 1b reveals the TEM micrographs of ZnO NR clusters with 40 and 60 nm diameters. The crystal simulations shows three major crystal indices, that is, (1 0 $\bar{1}$0), (0 0 0 2), and (1 0 $\bar{1}$ 1) that form the rod-like ZnO crystal facets [22, 23].

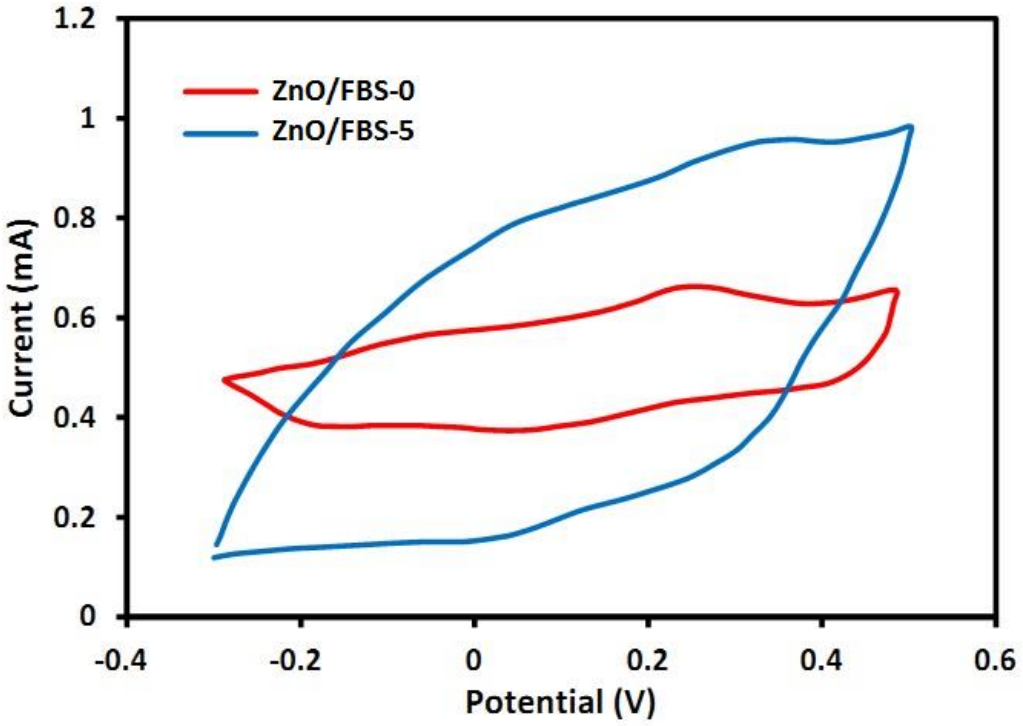

Figure 2. CV of FBS biocomposite incorporated by 0 wt% and 5 wt% content of ZnO nanorods at a 30 mVs^{-1} scan rate.

CV analysis was done to consider the capacitance of FBS biocomposite incorporated by various content of ZnO nanorods. The capacitive performance of biopolymer including 0 wt% and 5 wt% ZnO are shown in Figures 2. The redox processes were not recognized in the potential region [24, 25]. This result confirms the improvement of electrochemical properties in FBS biopolymer incorporated with ZnO nanorods. Furthermore, the higher conductivity of biocomposite incorporated by ZnO nanostructures (Fig. 2) reveals more charge carriers into the nanocomposites which may increase the antibacterial property of starch-based biocomposite by the electrostatic discharge between bacteria and ZnO nanorods[26, 27]. Thus, the ZnO/FBS nanopolymers can be used as antibacterial food packaging materials for proper food preservation.

The thermal stability of biocomposite matrixes is evaluated using TG analysis and compared with those of nonfiller starch polymer and ZnO/FBS nanocomposite films with various ZnO contents (Fig. 3). As the ZnO concentration increases, the nanocomposites reveal a significant postponement in weight loss at high temperatures above 150 °C. The first stage of thermal degradation (the temperature

ranges from 40 °C to 250 °C) is associated with the low molecular weight compounds that are mostly absorbed and bound to water.

The higher temperature stage, which exceeds 300 °C, may be ascribed to the thermal decomposition of more stable structures. At a weight loss of 50% during TGA, the temperature is increased from 264.5 °C to 337.3 °C with increasing ZnO concentration from 0wt% to 5wt%. This result can be related to the fact that ZnO NRs reduce the diffusion rate in volatile decomposition products outside the nanocomposite film. The thermal stability improvement of the films is mostly correlated to the dispersion and the thermal resistance of ZnO nanostructures in the FBS matrix [28]. Starch and ZnO can provide a stronger interaction in the nanocomposite films, and ZnO can act as a physical cross-linking to decrease the starch thermal decomposition. Furthermore, dispersive ZnO NRs are a very important barrier to preventing the release of weak FBS components. Therefore, the thermal degradation of the FBS can be retarded, and the thermal stability can be improved.

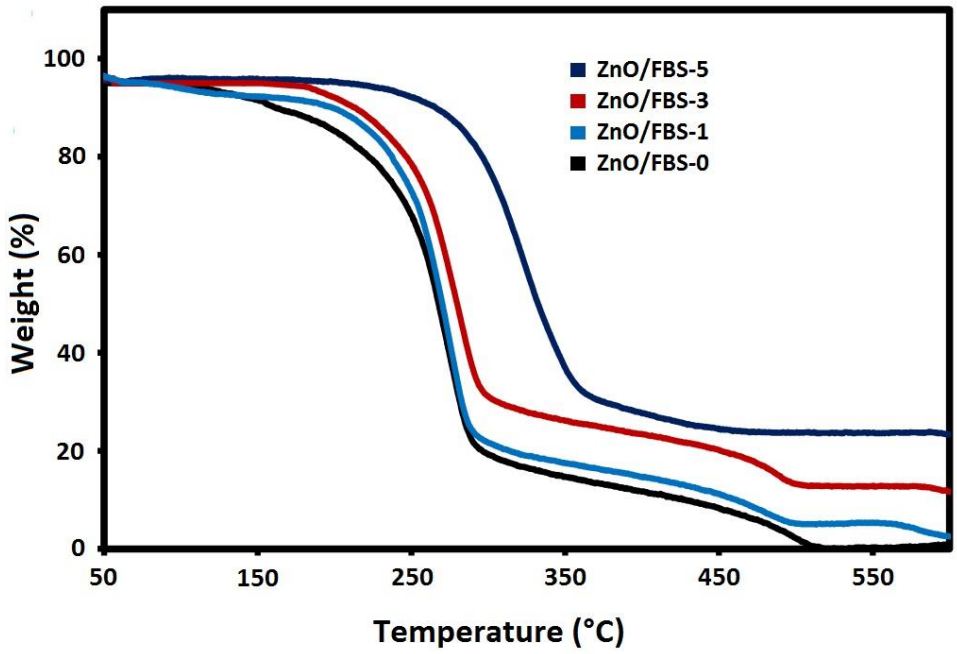

Figure 3. TGA curves of ZnO/FBS nanocomposite films with different ZnO content from 50 °C to 600 °C at a 10 °C/min rate under the N flow of 20 mL/min to prevent thermo-oxidative reactions.

Figure 4 shows the FESEM images of the ZnO/FBS nanocomposite matrix at various magnifications. ZnO NRs maintain their shape even after it's embedded into the FBS matrix. Few agglomerates of ZnO NRs appear in the ZnO/FBS nanocomposites with higher ZnO nanostructure content (ZnO/FBS-5).

Figure 5a shows the relative permittivity (ε_r) for different ZnO concentrations as a function of frequency at room temperature. It reveals a significant change as the ZnO nanofiller concentration is increased. A significant scattering of permittivity in the low frequency is obtained, then an almost frequency-independent behavior is observed above 10 kHz in all samples. ZnO nanofiller and plasticizer addition in nanocomposite films may lead to further charge carrier localization with mobile

ions. This phenomenon produces higher ε_r value with significant low frequency scattering. The decrease in ε_r with the increase in frequency can be associated with the electrical relaxation and material electrode polarization. Furthermore, the localization of charge carriers in the nanocomposites incorporated with ZnO NRs can be the reason for the enhancement of the antibacterial properties of starch-based polymer through the electrostatic discharge between ZnO NRs and bacteria [26].

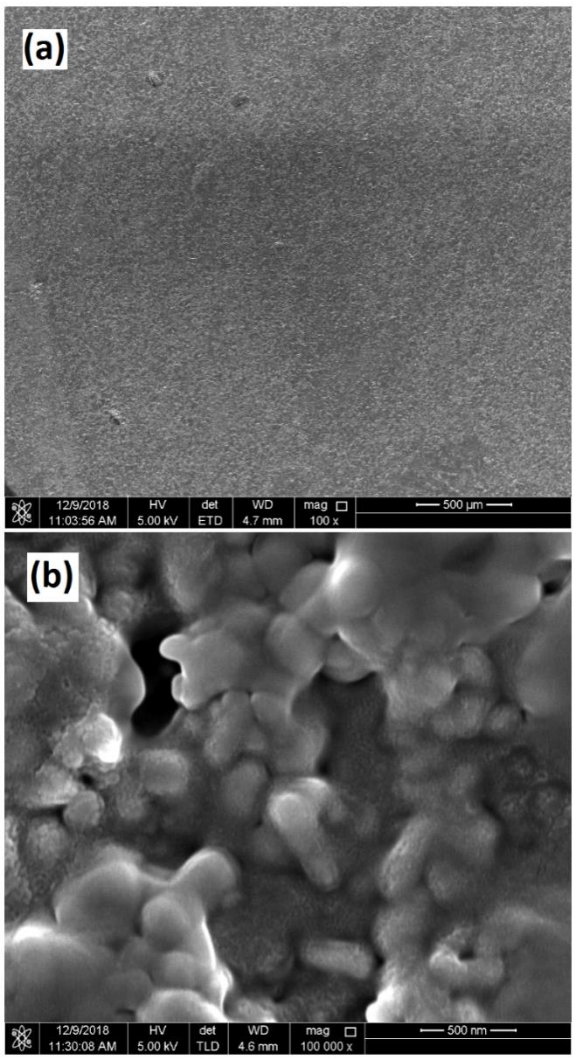

Figure 4. (a) and (b) FESEM images of ZnO/FBS-5 nanocomposite film with different magnification.

Figure 5b shows the variation in loss tangent (tanδ) with frequency at different ZnO contents in ZnO/FBS nanocomposite at room temperature. At low frequency regions, the tan δ of FBS film is higher compared with that of nanocomposite incorporated with ZnO. It is expected that tanδ values increase with increasing concentrations of the ZnO nanofiller in the composite film due to the charge transport by different interfaces or chain and defects. At lower filler loading, the amount of nanofiller present in nanocomposite film is lower. Thus, less free charge carriers from filler are available in ZnO/FBS nanocomposite. In this case, the interparticle spacing is high that may result in higher charge trapping sites and reduce the conducting path. These conditions increase the possibility of charge

neutralization and trapping. The tanδ obtained is similar to or less than that of the FBS matrix at lower nanofiller loading. Meanwhile, nanocomposite film with higher ZnO concentration will result in higher free charge carriers, which can decrease the interparticle spacing of nanofiller and decrease the charge trapping sites and probability of charge neutralization, to accumulate in the ZnO/FBS matrix.

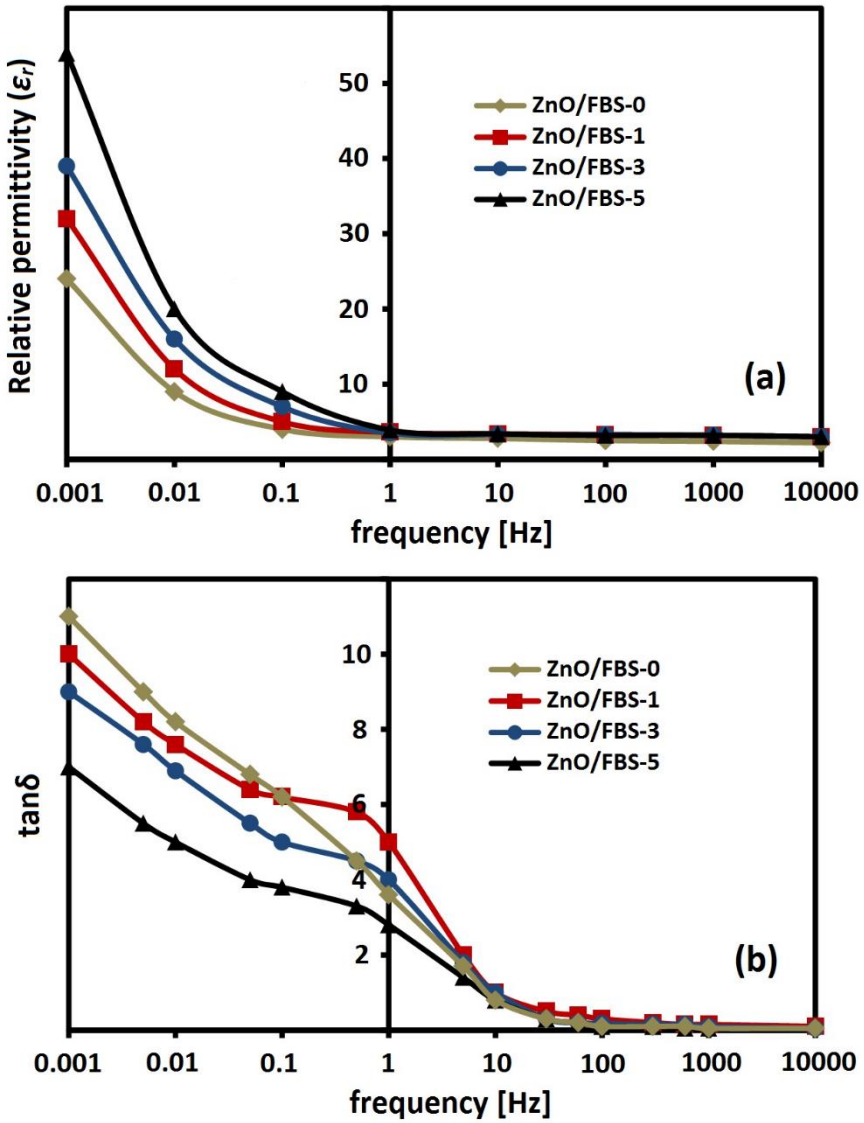

Figure 5. Frequency response of (a)relative permittivity and (b) loss tangent for different concentration of ZnO in the frequency range between 0.001 and 10000 Hz at room temperature.

Therefore, higher electrical conduction behavior of ZnO/FBS nanocomposite matrix will be obtained. These conditions result in significantly smaller tanδ of the ZnO/FBS nanocomposite matrix than that of the FBS matrix.

However, few mechanisms have been proposed to explain changes in the antimicrobial activities of ZnO against gram-positive and negative bacteria, there is still little doubt. Hence, further studies are needed to explain the susceptibility of these microorganisms to the ZnO nanostructures. The antibacterial activity of FBS film and ZnO/FBS nanocomposite have been verified against *E. coli*

and *S. aureus*. As shown in Fig. 6, all nanocomposite samples incorporated with ZnO nanorods show strong antibacterial activities with the increase in concentration ZnO nanorods.

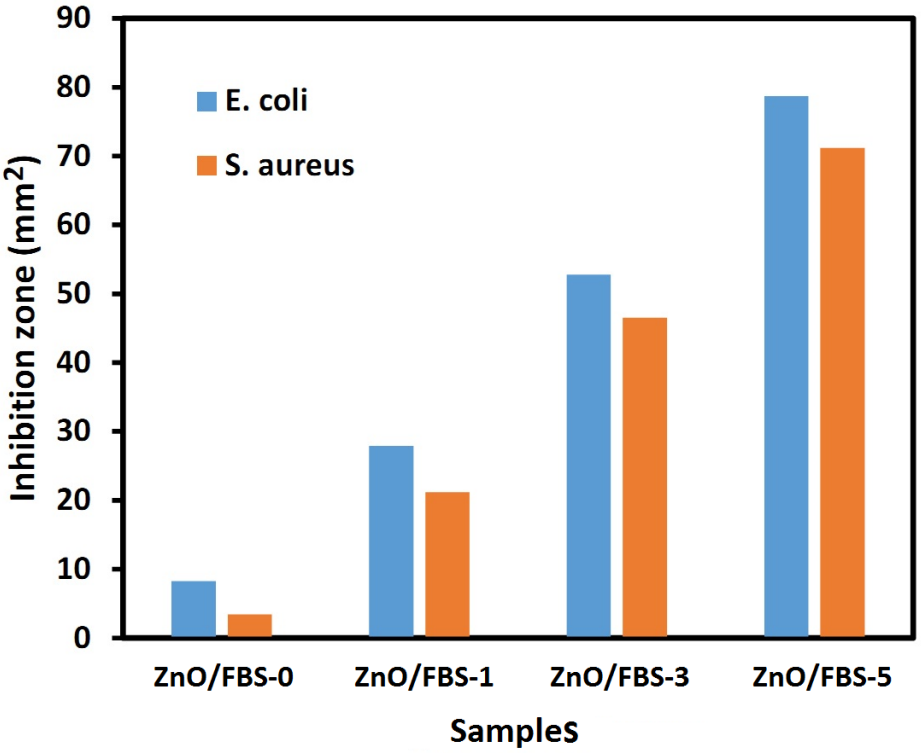

Figure 6. Effect of ZnO NRs concentration on antimicrobial activity of ZnO/FBS nanocomposite films using inhibition in a solid media zone

The results exhibit that the ZnO/FBS-5 nanocomposite sample has the excellent antimicrobial activity among the other samples tested. Moreover, *E. coli* has a greater sensitivity to ZnO/FBS nanocomposite compared to *S. aureus*. The high resistance of *S. aureus* in ZnO nanorods than that of *E. coli* can be related to the changes among these two bacteria due to the intracellular antioxidant contents, such as carotenoid pigments within *S. aureus* [29].

Table 1. Overview of inhibition zone of biopolymer films incorporated with ZnO nanostructures

Biopolymer materials	**Nanostructures**	**Inhibition zone (mm^2)**		**Ref.**
		S. aureus	**E. coli.**	
Soluble soybean polysaccharide	TiO_2 nanoparticles	71	53	[30]
Corn starch	Menthapulegium oil	83	76	[31]
Poly(vinyl chloride)-based Film	ZnO nanoparticles	58	63	[32]
Alginate	Cinnamon Essential Oil Nanoemulsions	48	45	[33]
Fava bean starch	ZnO nanorods	71	78	This work

Excellent antimicrobial activity of ZnO nanostructures against *S. aureus* and *E. coli* and the corresponding mechanism of action have also been demonstrated by other researchers. Table 1

indicates the inhibition zone of biopolymer films incorporated with nanostructures according to previous researches [30-33]. The functional activity of nanostructures is strongly influenced by their sizes [34]. Thus, the antimicrobial activity of ZnO nanorods on *E. coli* and *S. aureus* can be enhanced with the aspect ratio of nanofillers. This phenomenon can be related to the surface area/volume ratio, which concludes in the increased reactivity of the ZnO surface in nm size [35]. Given that the H_2O_2 generation relies more on the ZnO surface area, the larger surface area will conclude in more reactive oxygen species on the ZnO surface, thereby resulting in better antibacterial activity and higher aspect ratio. The presence of H_2O_2 leads to a reduction in bacterial growth, which can be a dominant mechanism for antibacterial behaviour [36].

4. CONCLUSIONS

ZnO/FBS bionanocomposites were produced using incorporating ZnO NRs into plasticized starch. The thermal stability improvement of the films is mostly correlated to the dispersion and the thermal resistance of ZnO nanostructures in the FBS matrix. ZnO nanofiller and plasticizer addition in nanocomposite films may lead to further charge carrier localization with mobile ions which enhance the antibacterial properties of starch-based polymer through the electrostatic discharge between ZnO NRs and bacteria. The peak appearance for any concentration in the loss tangent suggested the presence of relaxing dipoles in ZnO/FBS nanocomposite films. The strong interaction between the ZnO nanofiller and FBS matrix assisted in the improvement of biopolymer activities. ZnO/FBS biopolymer films revealed excellent antimicrobial activities against E. coli and S. aureus. Hence, ZnO/FBS nanocomposites have outstanding potential applications in food packaging.

References

1. T.S. Pandya, M.J. Dave, J. Street, C. Blake and B. Mitchell, *International Wood Products Journal*, 10(2019)22.
2. H. Karimi-Maleh, K. Cellat, K. Arıkan, A. Savk, F. Karimi and F. Şen, *Materials Chemistry and Physics*, 250(2020)123042.
3. J. Muller, C. González-Martínez and A. Chiralt, *Materials*, 10(2017)952.
4. F. Masmoudi, A. Bessadok, M. Dammak, M. Jaziri and E. Ammar, *Environ. Sci. Pollut. Res.*, 23(2016)20904.
5. Y.A. Salman, O.G. Abdullah, R.R. Hanna and S.B. Aziz, *International Journal of Electrochemical Science*, 13(2018)3185.
6. J. Rouhi, S. Mahmud, N. Naderi, C.R. Ooi and M.R.J.N.r.l. Mahmood, *Nanoscale Res. Lett.*, 8(2013)364.
7. A.S. Abreu, M. Oliveira, A. de Sá, R.M. Rodrigues, M.A. Cerqueira, A.A. Vicente and A. Machado, *Carbohydr. Polym.*, 129(2015)127.
8. E. Omidinia, S.M. Naghib, A. Boughdachi, P. Khoshkenar and D.K. Mills, *International Journal of Electrochemical Science*, 10(2015)6833.
9. A. Sorrentino, G. Gorrasi and V. Vittoria, *Trends Food Sci. Technol.*, 18(2007)84.
10. J. Rouhi, S. Mahmud, S.D. Hutagalung and S. Kakooei, *Journal of Micro/Nanolithography, MEMS, and MOEMS*, 10(2011)043002.
11. P. Kanmani and J.-W. Rhim, *Carbohydr. Polym.*, 106(2014)190.

12. H. Liu, J. Song, S. Shang, Z. Song and D. Wang, *ACS Appl. Mater. Interfaces*, 4(2012)2413.
13. N. Saba, P.M. Tahir and M. Jawaid, *Polymer*, 6(2014)2247.
14. N. Vigneshwaran, S. Kumar, A. Kathe, P. Varadarajan and V. Prasad, *Nanotechnology*, 17(2006)5087.
15. M. Beheshti, M. Che Ismail, S. Kakooei, S. Shahrestani, *Corros. Rev.*., 38(2020)1.
16. M. Azarang, A. Shuhaimi, R. Yousefi and S.P. Jahromi, *RSC Adv.*, 5(2015)21888.
17. Y.A. Arfat, S. Benjakul, T. Prodpran, P. Sumpavapol and P. Songtipya, *Food Hydrocoll.*, 41(2014)265.
18. M.G. Sari, M.R. Saeb, M. Shabanian, M. Khaleghi, H. Vahabi, C. Vagner, P. Zarrintaj, R. Khalili, S.M.R. Paran and B. Ramezanzadeh, *Prog. Org. Coat.*, 115(2018)143.
19. S.-K. Baek and K.B. Song, *LWT*, 89(2018)269.
20. J. Rouhi, M. Alimanesh, R. Dalvand, C.R. Ooi, S. Mahmud and M. Rusop, *Ceram. Int.*, 40(2014)11193.
21. H. Karimi-Maleh, F. Karimi, M. Alizadeh and A.L. Sanati, *The Chemical Record*, 20(2020)682.
22. M. Alimanesh, J. Rouhi and Z. Hassan, *Ceram. Int.*, 42(2016)5136.
23. R. Dalvand, S. Mahmud, J. Rouhi and C.R. Ooi, *Materials Letters*, 146(2015)65.
24. M. Beheshti, S. Kakooei, M. C. Ismail, S. Shahrestani. *Electrochim. Acta*, 341(2020) 1359762.
25. H. Karimi-Maleh, M. Sheikhshoaie, I. Sheikhshoaie, M. Ranjbar, J. Alizadeh, N.W. Maxakato and A. Abbaspourrad, *New Journal of Chemistry*, 43(2019)2362.
26. R. Baskaran, S. Selvasekarapandian, G. Hirankumar and M. Bhuvaneswari, *J. Power Sources*, 134(2004)235.
27. Z. Shamsadin-Azad, M.A. Taher, S. Cheraghi and H. Karimi-Maleh, *Journal of Food Measurement and Characterization*, 13(2019)1781.
28. P. Kumar, K. Sandeep, S. Alavi, V. Truong and R. Gorga, *J. Food Eng.*, 100(2010)480.
29. A. Sirelkhatim, S. Mahmud, A. Seeni, N.H.M. Kaus, L.C. Ann, S.K.M. Bakhori, H. Hasan and D. Mohamad, *Nano-Micro Lett.*, 7(2015)219.
30. T. Shaili, M.N. Abdorreza and N. Fariborz, *Carbohydr. Polym.*, 134(2015)726.
31. M. Ghasemlou, N. Aliheidari, R. Fahmi, S. Shojaee-Aliabadi, B. Keshavarz, M.J. Cran and R. Khaksar, *Carbohydr. Polym.*, 98(2013)1117.
32. X. Li, Y. Xing, W. Li, Y. Jiang and Y. Ding, Food Sci. Technol. *Int.*, 16(2010)225.
33. K. Frank, C.V. Garcia, G.H. Shin and J.T. Kim, *Int. J. Polym. Sci.*, 2018(2018)1.
34. N. Jones, B. Ray, K.T. Ranjit and A.C. Manna, *FEMS Microbiol. Lett.*, 279(2008)71.
35. M. Rai, A. Yadav and A. Gade, *Biotechnol. Adv.* , 27(2009)76.
36. W. Yin, J. Yu, F. Lv, L. Yan, L.R. Zheng, Z. Gu and Y. Zhao, *ACS nano*, 10(2016)11000.